Journal of Catalysis 257 (2008) 87–95

Contents lists available at ScienceDirect

Journal of Catalysis

www.elsevier.com/locate/jcat

Inorganic materials as supports for palladium nanoparticles: Application in the semi-hydrogenation of phenylacetylene

Sonia Domínguez-Domínguez, Ángel Berenguer-Murcia, Ángel Linares-Solano, Diego Cazorla-Amorós *

Carbon Materials and Environment (CME), Departamento de Química Inorgánica, Universidad de Alicante, Apartado 99, San Vicente del Raspeig, E-03080, Alicante, Spain

ARTICLE INFO

Article history:
Received 28 February 2008
Revised 14 April 2008
Accepted 14 April 2008
Available online 20 May 2008

Keywords:
Heterogeneous
Nanoparticles
Selective hydrogenation
Phenylacetylene
Styrene

ABSTRACT

A series of palladium heterogeneous catalysts supported on different inorganic materials were prepared using a palladium colloid and four different supports: γ-alumina (Pd/Al_2O_3), zeolite Beta (Pd/Beta), MCM-41, and Al-MCM-41. The two last catalysts were synthesized by two different methods of deposition of the metallic nanoparticles: impregnation or in situ synthesis of MCM in the presence of the Pd colloid. These catalysts were evaluated in the partial hydrogenation of phenylacetylene, performed in liquid phase, under very mild conditions (323 K, H_2 flow of 30 mL/min, 1 bar pressure). All of the catalysts had very high selectivity toward styrene (around 96%) after total conversion. The activity values were very close to those of the homogeneous catalysts, being much greater for the catalysts obtained by synthesis of the MCM materials in presence of the Pd colloid, for which, the TOF values were fourfold to sixfold greater. The catalysts proved to be reusable; neither the catalytic activity nor the selectivity decreased appreciably after five consecutive cycles of reaction. Moreover, inductively coupled plasma (ICP) analysis confirmed that no Pd leaching from the samples occurred during the catalytic reaction.

1. Introduction

Partial reduction (i.e., semihydrogenation) of phenylacetylene is a reaction of industrial importance. This compound is an unwanted feedstock component in polystyrene production plants, and its removal to levels below 10 ppm is mandatory to avoid poisoning of the polymerization catalyst. Furthermore, partial reduction of phenylacetylene is a very convenient process for catalyst optimization, because it enables both evaluation of process design [1] and quick testing of hydrogenation catalysts [2] under very mild conditions.

For practical reasons, heterogeneous catalysts are highly significant in modern industry. Their numerous advantages include immobilization of the catalytic species on a suitable support, which avoids agglomeration of the active species during chemical reaction, enables easy catalyst recovery (and thus easy product separation), and greatly simplified catalyst handling. It must be noted, however, that the choice of a suitable support is very important, because the interaction with the active phase may play a critical role in the final performance of the catalysts [3,4].

During the last two decades, due to significant advancements in the development of porous materials, increasing attention has been focused on the use of inorganic materials (e.g., alumina, silica, zeolites) as supports for heterogeneous catalysts [5]. As a matter of fact, although zeolites have long since proved their great usefulness [6], one of their disadvantages is their lack of pores of sufficient size to perform host-guest reactions of relatively large molecules. The discovery of a siliceous material with regular pores of 2 nm in diameter arranged in a hexagonal fashion (MCM-41) [7] was a turning point in the development of materials for heterogeneous catalysts: the preparation of mesostructured solids.

In two previous papers [8,9], we reported that polymer-protected Pd-based nanoparticles were very promising catalysts in both homogeneous and heterogeneous phases for the synthesis of styrene from phenylacetylene under very mild conditions with very high selectivity. Our goal here is to extend this knowledge by depositing palladium nanoparticles on different inorganic supports in an attempt to identify the most desirable characteristics in these types of supports for optimizing the semihydrogenation reaction of phenylacetylene. To assess the relevance of the different properties of inorganic solids, we used four well-known catalytically active supports: a zeolite (zeolite Beta), γ-Al_2O_3, and two mesostructured materials (MCM-41 and Al-MCM-41). Furthermore, we used a novel synthesis method for Pd/MCM-41 and Pd/Al-MCM-41; in these catalysts, the mesostructured materials were synthesized in presence of the Pd nanoparticles. The prepared solids were thoroughly characterized and tested for their catalytic properties in the semihydrogenation of phenylacetylene under mild conditions. Here we critically compare the results with those available in the literature.

* Corresponding author. Fax: +34 965 903454.
E-mail address: cazorla@ua.es (D. Cazorla-Amorós).

0021-9517/$ – see front matter
doi:10.1016/j.jcat.2008.04.008

2. Experimental

2.1. Catalyst preparation

A series of supported catalysts were prepared by deposition of palladium nanoparticles onto the selected inorganic supports. The preparation of the colloidal Pd nanoparticles was carried out by the reduction by solvent process of the Pd precursor with ethylene glycol [palladium (II) acetate], as described previously [8,9]. After synthesis, the Pd colloid was purified with acetone and then redispersed in MeOH, so that the Pd concentration in the resulting Pd nanoparticles/methanol dispersion (mg Pd/mL solution) remained known. Four inorganic materials were used:

(1) The γ-Al_2O_3 support, in a powder form, was obtained from the milling of activated γ-aluminum oxide pellets, from Alfa Aesar (31268).
(2) The zeolite Beta, in the acidic form (H-Beta zeolite), was prepared by calcination of NH_4-Beta zeolite at 823 K for 8 h (SiO_2/Al_2O_3 molar ratio, 25) provided by Zeolyst (CP814E).
(3) MCM-41 and Al-MCM-41 were prepared following a synthetic procedure given in the literature [10,11], using hexadecyltrimethylammonium bromide (CTAB; Aldrich, 855820) as the template and tetraethylorthosilicate (TEOS; Aldrich, 131903) and sodium aluminate ($NaAlO_2$; Riedel-de Haën, 13404) as the Si and Al sources. Thus, in the synthesis of purely siliceous MCM-41, 4.8 g of CTAB was dissolved in 240 mL of distilled water. The mixture was stirred and heated gently until complete dissolution was achieved. Then 16 mL of NH_3 was added, and the resulting mixture was stirred at 380 rpm for 5 min. Subsequently, 20 mL of TEOS was added, and the solution stirred for 1 h. Afterward, the white solid was filtered off, washed with distilled water, dried overnight at 323 K, and finally calcined in air at 823 K for 5 h at a heating rate of 1 K/min, in a N_2 flow.
(4) Al-MCM-41 was prepared in the same way, but with $NaAlO_2$ added to the synthesis mixture (to obtain a SiO_2/Al_2O_3 ratio of 25) before the addition of NH_3.

The Pd nanoparticles were supported on the materials using the impregnation method. First, the appropriate volume of the palladium nanoparticles/methanol dispersion was mixed with the support. The catalysts were prepared so as to have a final catalyst loading of 1 wt%. The solution was then gently stirred at room temperature for 3 days. After this, the solution was transferred to an oven at 60 °C until the methanol was evaporated. The collected solid was washed with a mixture of ethanol and water (50/50%, V/V) several times. Finally, the resulting supported catalyst was dried overnight. The prepared catalysts are designated Pd/Al_2O_3, Pd/Beta, Pd/MCM-41, and Pd/Al-MCM-41.

For the MCM-41 and Al-MCM-41, we also used an alternative preparation method known as simultaneous synthesis (s.s.). The necessary volume of palladium nanoparticles/water dispersion was mixed with the solution of CTAB in distilled water; the remaining synthesis steps were the same as described previously. Thus, the MCM-41 and Al-MCM-41 were synthesized in the presence of Pd nanoparticles, designated Pd/MCM-41_s.s. and Pd/Al-MCM-41_s.s.

2.2. Characterization

N_2 and CO_2 adsorption measurements of the supports and the synthesized Pd-supported catalysts were performed at 77 K and 273 K, respectively, using a Micromeritics ASAP2020 system. Samples were degassed at 523 K under vacuum for 6 h. The specific surface areas, S_{BET}, were calculated from the BET equation. The external surface, S_{ext}, excluding the area corresponding to micropores, was calculated by de Boer's t-method [12]. The total micropore volume, V_{DRN_2}, was determined by applying the Dubinin–Radushkevich [13] equation to the N_2 adsorption isotherm, using a P/P_0 range of 0.005 to 0.14. The total pore volume, V_{total}, was obtained at $P/P_0 = 0.95$. The volume of mesopores with pore sizes between 2 and 7.5 nm, V_{meso}, was calculated by the difference between the volume of N_2 adsorbed at $P/P_0 = 0.7$ and $P/P_0 = 0.2$. The volume of narrow micropores, V_{DRCO_2}, was calculated from CO_2 adsorption at 273 K, using the DR equation and for relative pressures below 0.025. The average pore size, d_p, was calculated from V_{total} and S_{BET} using the following equation [10]:

$$d_p = 4 \cdot V_{total}/S_{BET}. \quad (1)$$

The densities of the adsorbed phases used for the calculations were 0.808 g/mL for N_2 and 1.023 g/mL for CO_2 [14].

The palladium content in the prepared catalysts was determined using inductively coupled plasma-optical emission spectroscopy (ICP-OES), in a Perkin–Elmer Optima 4300 ICP-OES spectrometer. Before analysis, the samples were treated in concentrated HNO_3 at 343 K for 48 h.

The catalysts were characterized by transmission electron microscopy (TEM) using a JEOL JEM-2010 high-tilt instrument operating at 200 kV with a structural spatial resolution of 0.5 nm. High-resolution TEM (HRTEM) studies were performed in a JEOL JEM-3011 electron microscope operating at 300 kV with a structural resolution of 0.16 nm. The samples were prepared by suspending the ground catalysts in ethanol and sonicating for 1 h. A drop of the suspension was deposited on a carbon-coated copper grid, followed by drying at ambient conditions. The average value of the palladium particle diameters (d_{TEM}) was calculated by the following equation:

$$d_{TEM} = \frac{\sum n_i d_i}{\sum n_i}, \quad (2)$$

where n_i ($n_i > 100$) is the number of particles of diameter d_i. The metal accessibility value (D_{TEM}) was estimated by assuming spherical particle geometry and using the following equation [15]:

$$D_{TEM} \approx 0.9/d_{TEM}\ (\text{nm}). \quad (3)$$

Metal dispersion (D_{CO}) and metal particle size (d_{CO}) also were determined by CO chemisorption with an automatic adsorption system (ASAP 2020 Chemisorption provided by Micromeritics). CO chemisorption was carried out at 308 K in the pressure range of $0.8–65 \times 10^4$ Pa. Using the difference between the total and the reversible chemisorbed CO, the number of exposed Pd metal atoms was calculated, assuming a chemisorption stoichiometry of Pd/CO = 2 [16–18]. The mean particle diameter obtained by chemisorption of CO, d_{CO}, was determined using the same equation used for the calculations in TEM analyses [Eq. (3)].

2.3. Catalytic reactions

The liquid-phase hydrogenation of phenylacetylene was performed as described previously [8]. These catalytic tests were carried out in a 250-mL three-necked flask at a temperature of 323 K, a H_2 flow of 30 mL/min, and a total pressure of 1 bar. Stirring was done at 800 rpm with a magnetic stirring bar, to prevent mass transport limitations. In a typical catalytic experiment, the total volume was 100 mL, with 10 mL (0.089 mol) of phenylacetylene, with methanol used as the solvent. The reactant:Pd molar ratio was always set to 7300. All reactions were performed up to 100% conversion. Samples were removed at regular intervals and diluted to a 1:100 ratio with methanol. The liquid reactants and products were analyzed by gas chromatography (GC), using a HP 6890 Series II chromatograph equipped with a HP-1 cross-linked methyl

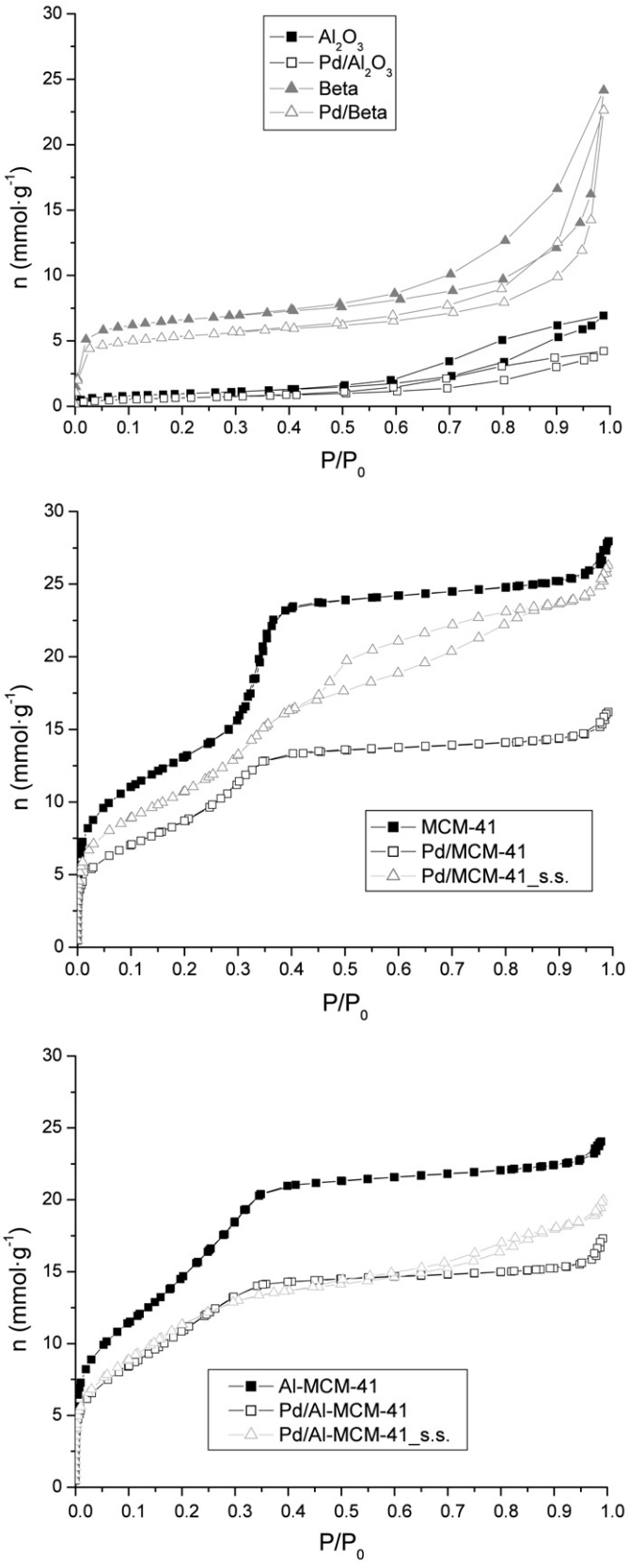

Fig. 1. Nitrogen adsorption–desorption isotherms at 77 K of supports and prepared Pd-supported catalysts.

siloxane capillary column (30 m × 250 μm × 0.25 μm) and a flame ionization detector. The catalytic activity was characterized by the turnover frequency (TOF) and selectivity toward styrene.

Table 1
Surface area characterization results for supports and prepared Pd-supported catalysts

Sample	S_{BET} (m^2/g)	S_{ext} (m^2/g)	$V_{DR\,N_2}$ (cc/g)	V_{total} (cc/g)	V_{meso} (cc/g)	$V_{DR\,CO_2}$ (cc/g)	d_p (nm)
Al_2O_3	78	78	0.04	0.20	0.08	0.05	10.3
Pd/Al_2O_3	54	54	0.02	0.12	0.05	0.05	8.9
Beta	460	240	0.24	0.49	0.31	0.15	4.3
Pd/Beta	390	206	0.19	0.41	0.25	0.14	4.2
MCM-41	1045	59	0.44	0.87	0.83	0.16	3.3
Pd/MCM-41	875	60	0.33	0.59	0.56	0.10	2.7
Pd/MCM-41_s.s.	970	272	0.40	0.94	0.80	0.17	3.9
Al-MCM-41	1297	52	0.50	0.76	0.72	0.19	2.3
Pd/Al-MCM-41	928	43	0.38	0.52	0.51	0.13	2.2
Pd/Al-MCM-41_s.s.	1066	164	0.39	0.70	0.60	0.15	2.6

Finally, reuse of some of the samples (Pd/Al_2O_3, Pd/Beta, Pd/MCM-41_s.s., and Pd/Al-MCM-41_s.s.) was investigated, in terms of activity and selectivity, in five consecutive reactions.

3. Results and discussion

3.1. Catalyst characterization

N_2 adsorption isotherms of the inorganic materials before and after the support of Pd nanoparticles are shown in Fig. 1. As can be seen, Al_2O_3 and Pd/Al_2O_3 followed a type II isotherm, reflecting the monolayer–multilayer adsorption, according to the IUPAC classification [19–21]. These materials have some mesopores and practically no micropores [22]. The nitrogen adsorption–desorption isotherms for the zeolite H-Beta and the Pd/Beta (Fig. 1) were of type IV with a small hysteresis loop at high relative pressures indicative of capillary condensation in mesopores and a steep increase at low relative pressures related to the presence of micropores [20].

The nitrogen adsorption–desorption isotherms obtained with MCM-41, Pd/MCM-41, and Pd/MCM-41_s.s. samples and the respective samples with Al were all very similar. The isotherms showed a typical type IV adsorption isotherm [23–25] and displayed a sudden increase in the amount adsorbed in the range of relative pressures, P/P_0, of 0.3–0.4, characteristic of mesoporous materials having cylindrical pores with narrow pore size distribution. The pore size distribution was broader in the Al-containing samples. Moreover, the isotherms of N_2 of Pd/MCM-41_s.s. and Pd/Al-MCM-41_s.s. samples exhibited hysteresis loops at higher relative pressures, indicating an even broader pore size distribution for these materials.

The textural properties (S_{BET}, S_{ext}, $V_{DR\,N_2}$, V_{total}, V_{meso}, $V_{DR\,CO_2}$, and d_p) of the inorganic materials before and after the support of Pd nanoparticles are summarized in Table 1. According to these data, the specific surface area of the samples with the supported Pd nanoparticles (Pd/Al_2O_3, Pd/Beta, Pd/MCM-41, Pd/MCM-41_s.s., Pd/Al-MCM-41, and Pd/Al-MCM-41_s.s.) decreased compared with that of the corresponding support. The MCM samples that were synthesized in the presence of the Pd nanoparticles (Pd/MCM-41_s.s. and Pd/Al-MCM-41_s.s.) exhibited the smallest decrease in specific surface area, but at the same time, the textural properties of these two materials, as well as their larger average pore size (Table 1) and shape of the N_2 adsorption isotherms (Fig. 1), were not typical of the structure of MCM materials.

The results of the ICP analysis for the Pd content of the prepared catalysts are given in the first column of Table 2. It can be seen that the desired 1 wt% of Pd loading was not really achieved and that the amount of Pd deposited was around 0.7 wt% for all of the catalysts except zeolite Beta, for which it was nearly 0.9 wt%, probably due to the surface roughness of this material [26], which favors anchorage of nanoparticles. The rest of the metal (up to the 1 wt% of the initial synthetic procedure) was lost during the

synthesis procedure, and any insufficiently bound Pd nanoparticles were washed off the support, as we recently reported in Pd/C catalysts [9].

The metal dispersion of synthesized supported Pd catalysts was characterized by TEM and HRTEM analyses. Fig. 2 shows TEM micrographs of (a) Pd/Al_2O_3, (b) Pd/Beta, (c) Pd/MCM-41, (d) Pd/Al-MCM-41, (e) Pd/MCM-41_s.s. (before calcination), (f) Pd/MCM-41_s.s. (after calcination), (g) Pd/Al-MCM-41_s.s. (before calcination), and (h) Pd/Al-MCM-41_s.s. (after calcination). The obtained average particle sizes were as follows: (a) 2.1 ± 0.6 nm, (b) 2.4 ± 0.5 nm, (c) 2.5 ± 0.7 nm, (d) 2.4 ± 0.7 nm, (e) 5.7 ± 2.0 nm, (f) 6.8 ± 2.7 nm, (g) 5.1 ± 1.5 nm, and (h) 7.6 ± 2.7 nm. These particle sizes are very similar to the average particle size of Pd nanoparticles present in suspension in the colloid (2.4 ± 0.5 nm [8]), except in catalysts Pd/MCM-41_ss and Pd/Al-MCM-41_s.s., where the particles seemed to agglomerate during the synthesis of the materials and also to grow during the calcination step. Pd average particle size and metal dispersion results obtained from TEM anal-

Table 2
Pd content (wt%) by ICP analysis, and CO chemisorption and TEM characterization results of the prepared catalysts

Sample	Pd (wt%)	Particle size, d_{TEM} (nm)	Dispersion, D_{TEM}	Dispersion, D_{CO}	Metallic surface area (m^2/g_{cat})	Metallic surface area (m^2/g_{Pd})	Particle size, d_{CO} (nm)
Pd/Al_2O_3	0.62	2.10	0.43	0.30	0.84	135	3.00
Pd/Beta	0.84	2.42	0.37	0.30	1.12	134	3.00
Pd/MCM-41	0.69	2.46	0.37	0.32	0.98	141	2.81
Pd/MCM-41_s.s.[a]	0.77	6.82	0.13	0.08	0.27	35	11.25
Pd/Al-MCM-41	0.67	2.35	0.38	0.29	0.87	129	3.10
Pd/Al-MCM-41_s.s.[a]	0.60	7.61	0.12	0.07	0.22	33	12.86

[a] After calcination.

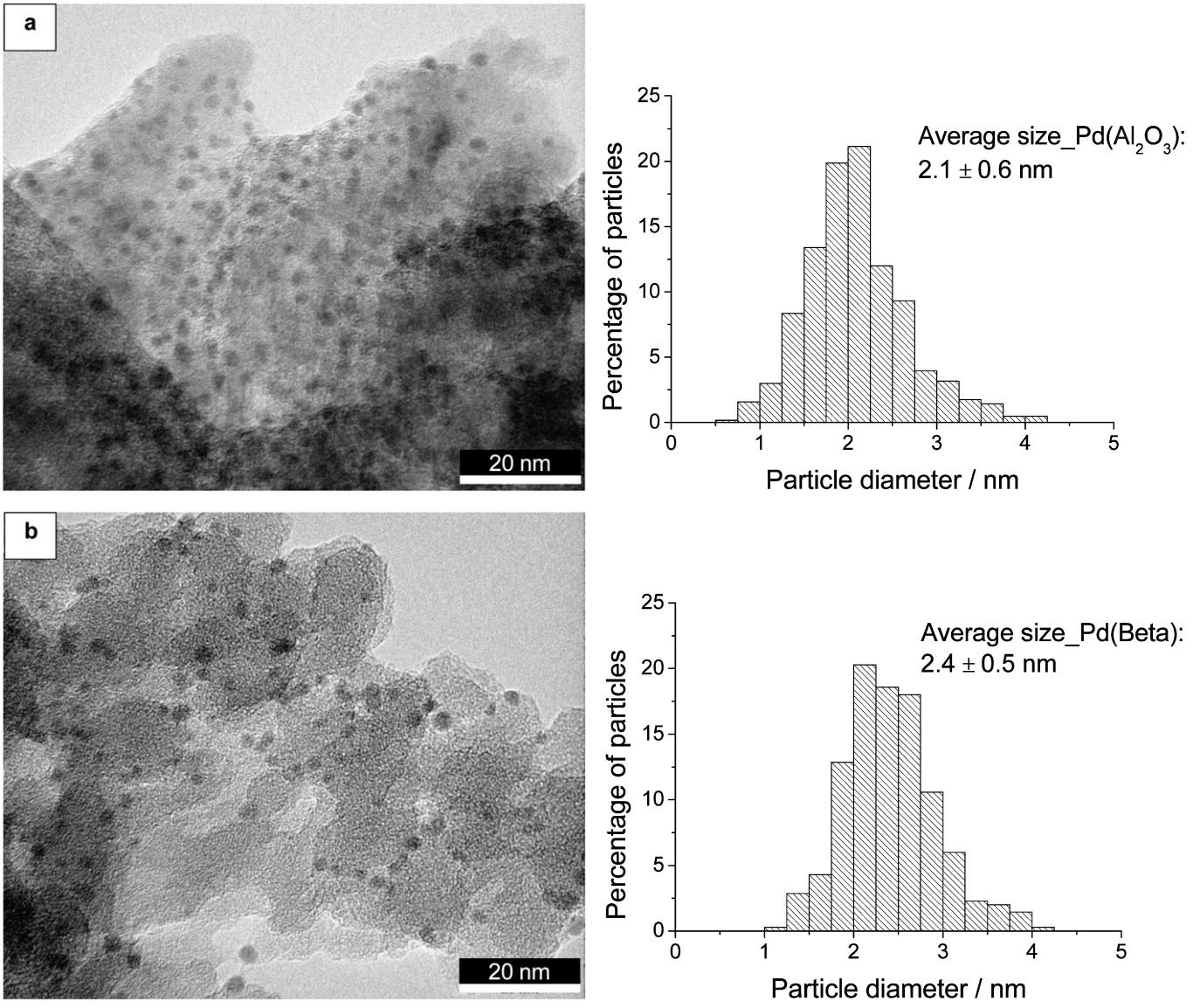

Fig. 2. TEM micrograph and their corresponding histograms of particles size of the different supported Pd catalysts: (a) Pd/Al_2O_3, (b) Pd/Beta, (c) Pd/MCM-41, (d) Pd/Al-MCM-41, (e) Pd/MCM-41_s.s. (before calcination), (f) Pd/MCM-41_s.s. (after calcination), (g) Pd/Al-MCM-41_s.s. (before calcination), and (h) Pd/Al-MCM-41_s.s. (after calcination).

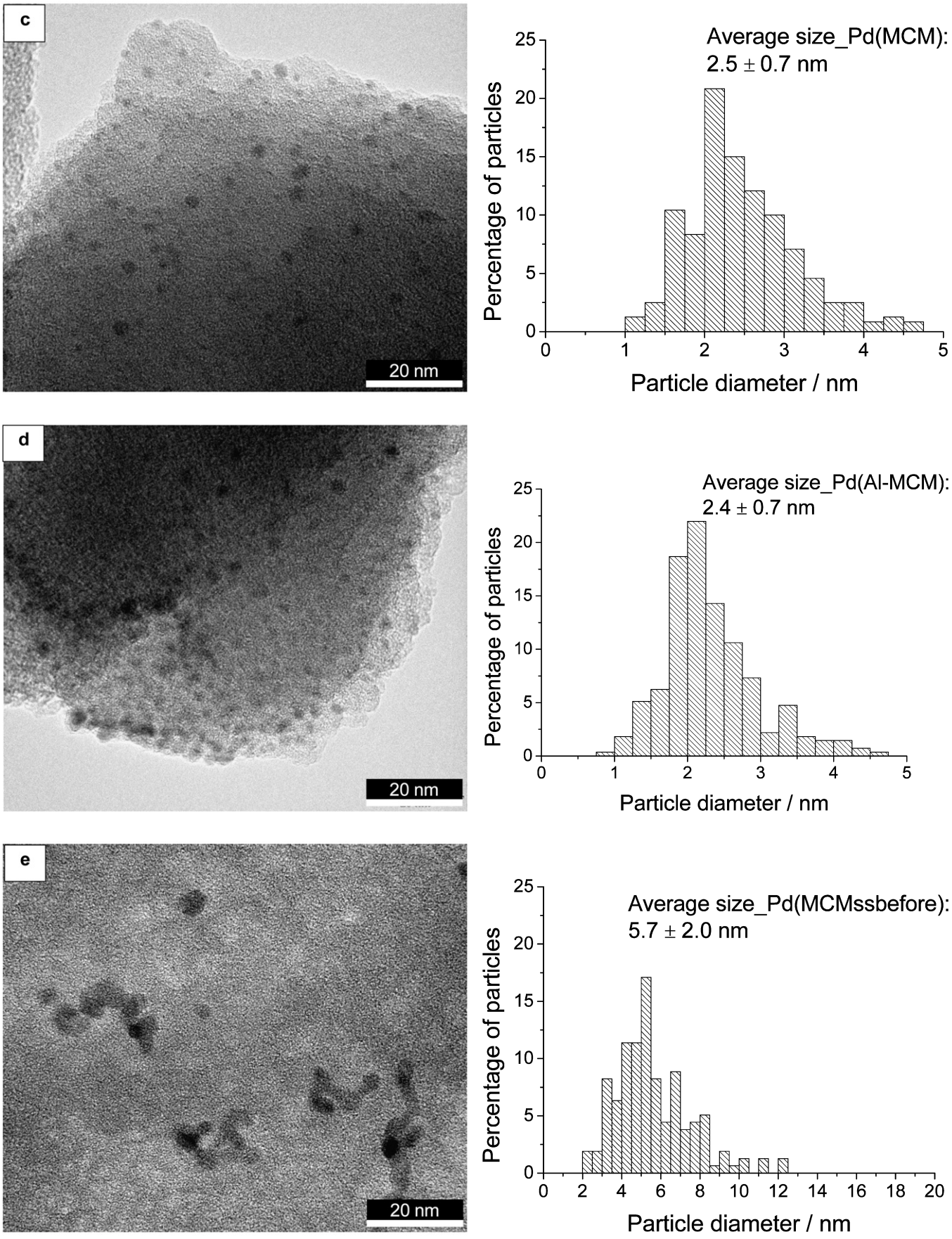

Fig. 2. (*continued*)

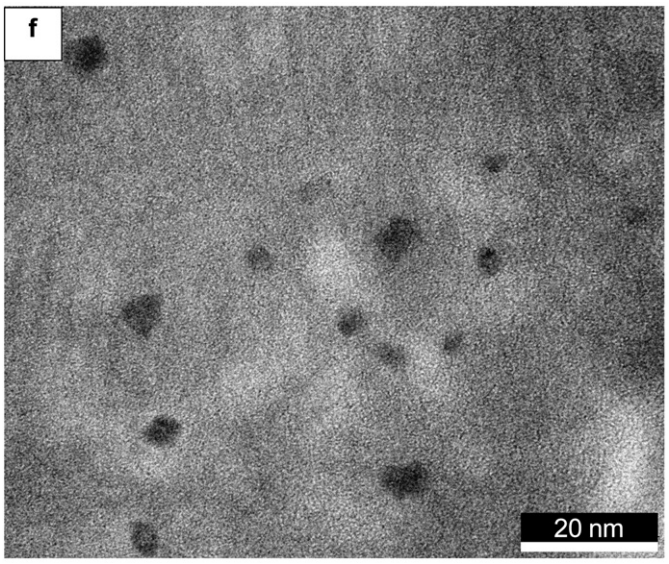

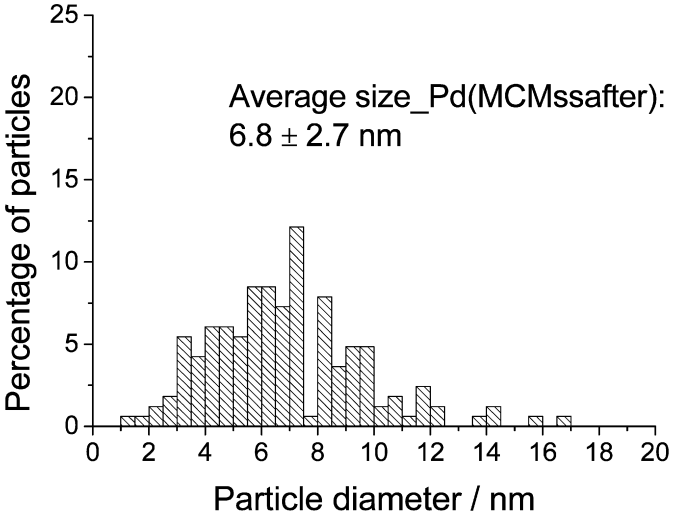

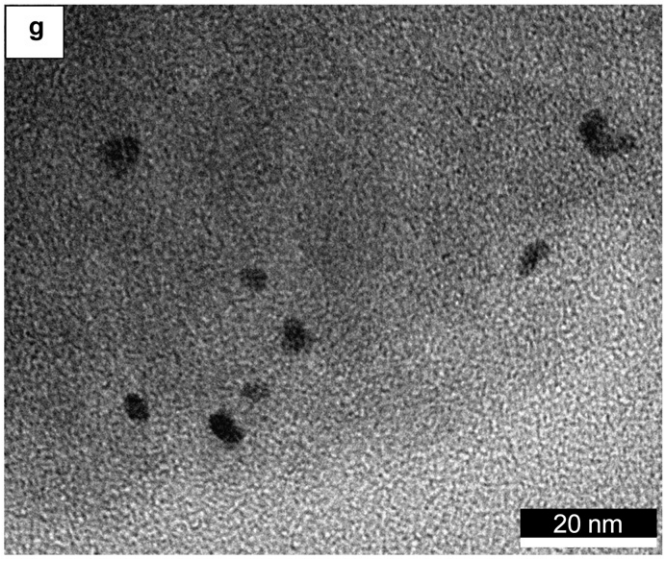

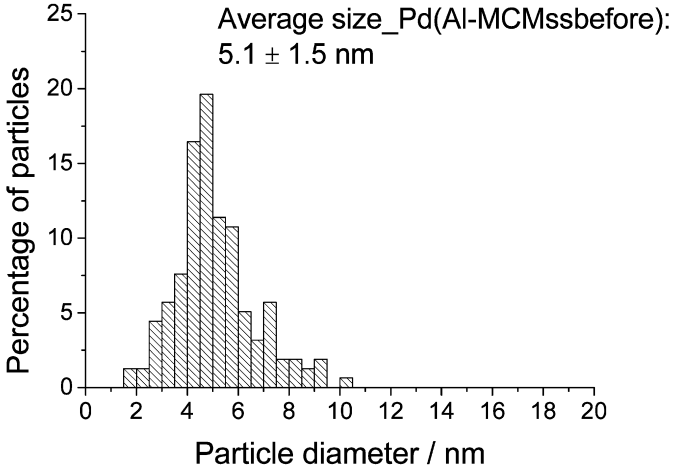

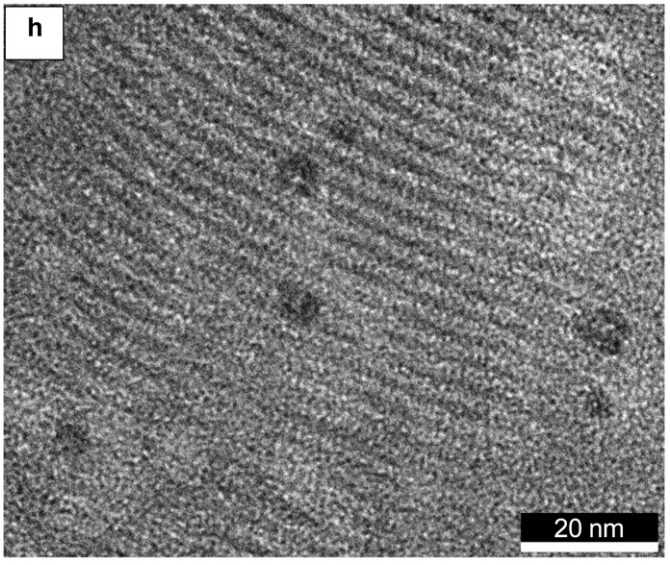

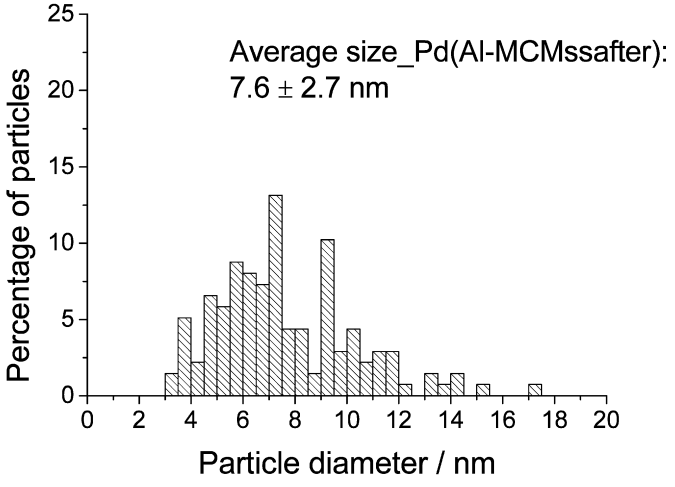

Fig. 2. (*continued*)

yses are given in the second and third columns, respectively, of Table 2.

A closer inspection of Figs. 2e–2h (s.s. materials) reveals some sections in which there seem to be areas around the nanoparticles with a sparser presence of inorganic matrix. This indicates that for the s.s. materials, in which the synthesis of the mesostructured phase occurs in the presence of the Pd nanoparticles, the molecules of surfactant may surround the individual nanoparticles (or clusters of nanoparticles), thus creating "pockets" within the silica-alumina matrix. These pockets provide a volume of available free space around the resulting nanoparticles, which provides a certain degree of freedom once the template has been removed by calcination.

As can be observed in the HRTEM micrographs, obtained from a higher magnification of the samples of Fig. 2, the synthesized nanoparticles of Pd/MCM-41 (Fig. 3a1) were essentially spherical; this result was also found for the rest of the catalysts. But in Pd/MCM-41_s.s. (Fig. 3b1), the nanoparticles were irregularly shaped and agglomerated. This also was observed in Pd/Al-MCM-41_s.s. The synthesized nanoparticles are of high crystallinity, as shown in Figs. 3a2 (Pd/MCM-41) and 3b2 (Pd/MCM-41_s.s). On the other hand, HRTEM results also demonstrated a better-defined pore structure orientation in Pd/MCM-41 (Fig. 3a), in which the support was synthesized without the presence of the Pd nanoparticles. In Pd/MCM-41_s.s. (Fig. 3b), the solid had less order in the structure and slightly larger pores.

The fraction of exposed Pd in the catalysts (D_{CO}) and the mean Pd particle size (d_{CO}) were calculated from the irreversible CO chemisorption experiments. The results are summarized in the last four columns of Table 2. The Pd particle sizes determined by this technique were slightly larger than those detected by TEM analysis in all of the catalysts except Pd/MCM-41_s.s. and Pd/Al-MCM-

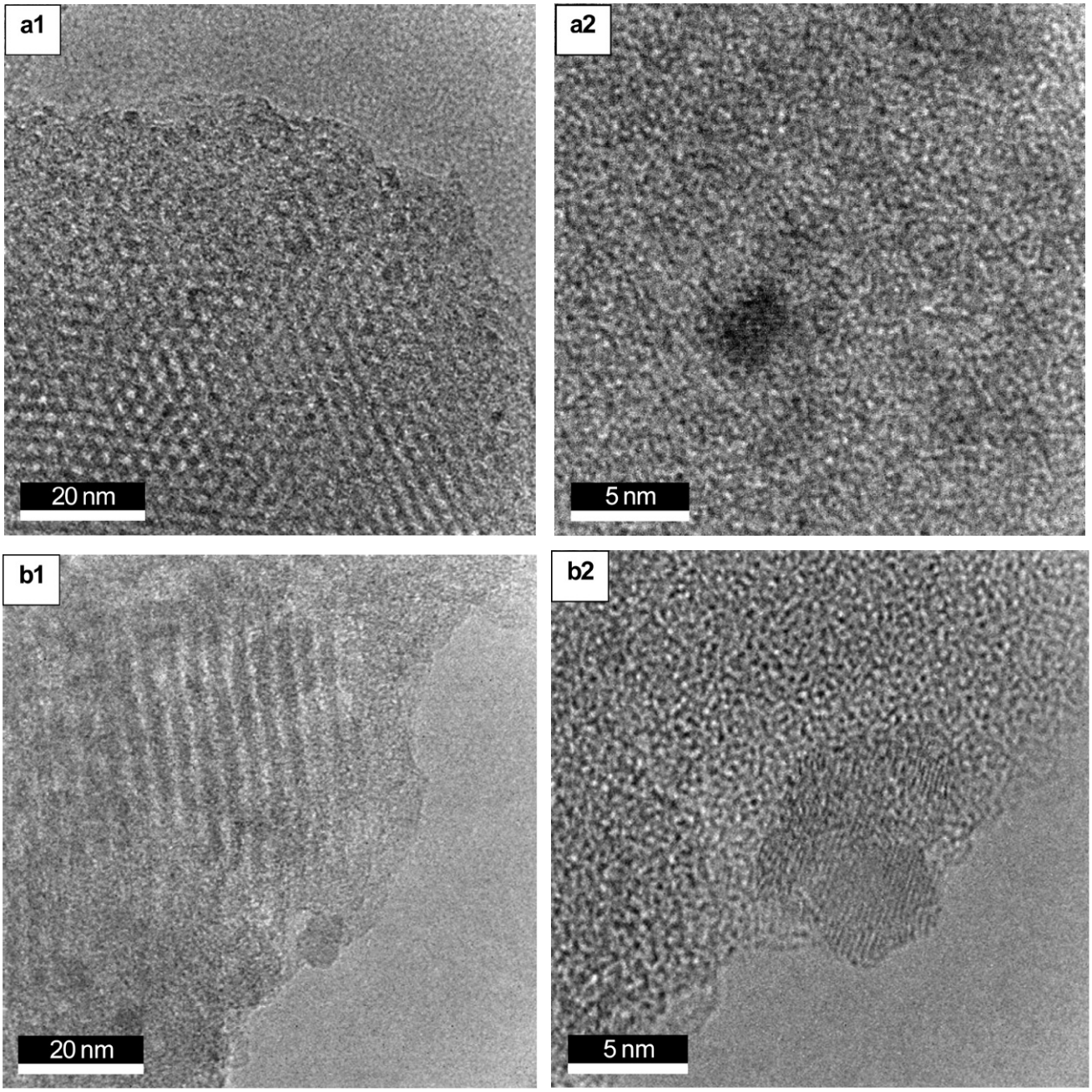

Fig. 3. HRTEM micrograph of samples: (a) Pd/MCM-41, (b) Pd/MCM-41_s.s.

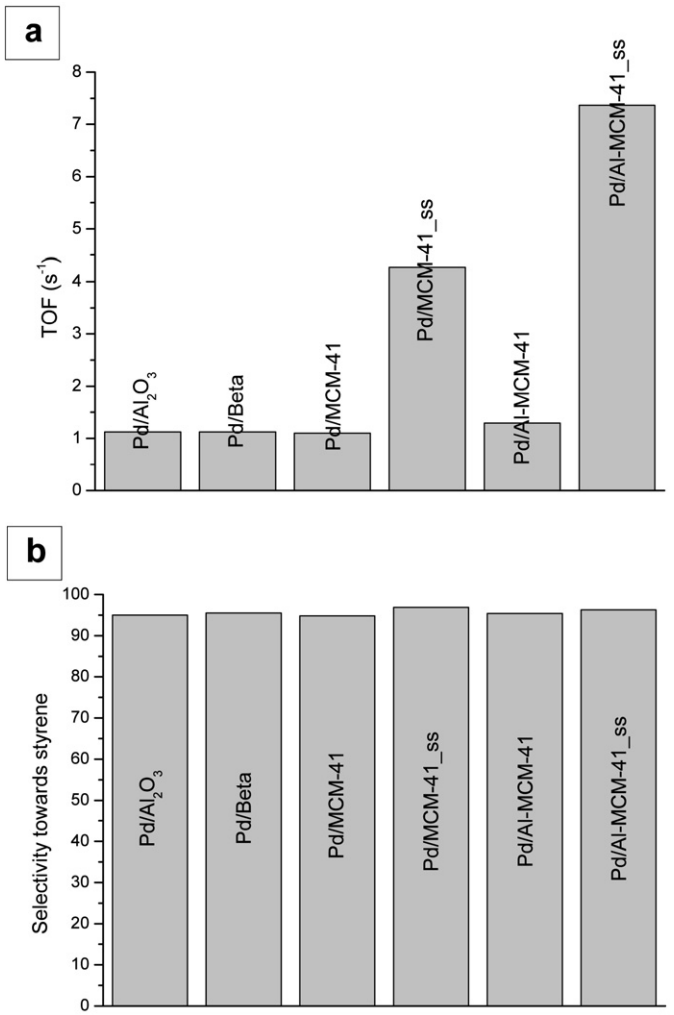

Fig. 4. (a) TOF and (b) selectivity towards styrene of the 6 catalysts in the first cycle of hydrogenation of phenylacetylene.

41_s.s., which exhibited much larger Pd particles. Thus, the accessible sites of the Pd particles to the molecule of CO were smaller than the value determined by TEM, especially in the latter two catalysts, in which the nanoparticles are confined in the material. We used the results obtained by CO chemisorption to calculate catalytic activity.

3.2. Catalytic tests

We used the activity in the hydrogenation of phenylacetylene as the catalytic test for the synthesized materials. The reaction was performed as outlined in Section 2, using the same conditions as used in previous work [8,9] to allow meaningful comparisons of results.

Fig. 4 shows TOF and selectivity results from the first cycle of catalytic testing for our six catalysts under our experimental conditions. TOF values were obtained by dividing the reaction rates by the number of palladium sites per gram of catalyst (calculated by CO chemisorption analysis). Selectivity was referred to the desired product (styrene). As can be observed, the Pd-supported catalysts exhibited very similar catalytic properties in the semihydrogenation of phenylacetylene, except Pd/MCM-41_s.s. and Pd/Al-MCM-41_s.s.. Total conversion, also with very high selectivity toward styrene (around 96%), was achieved for all samples. The activity values were very close to those of the homogeneous catalyst (TOF = 1.01 s^{-1}) [8] for all catalysts except Pd/MCM-41_s.s. and

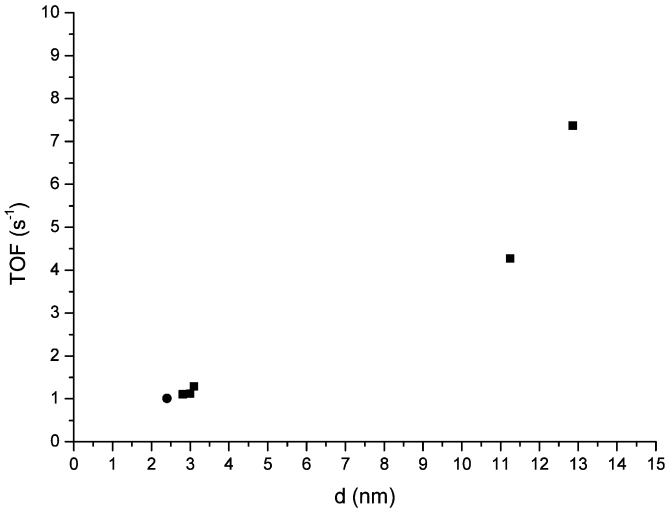

Fig. 5. Relation between particle diameters and TOF in the first cycle of hydrogenation of phenylacetylene of the different catalysts of this study (■) and colloidal Pd nanoparticles (●) [8].

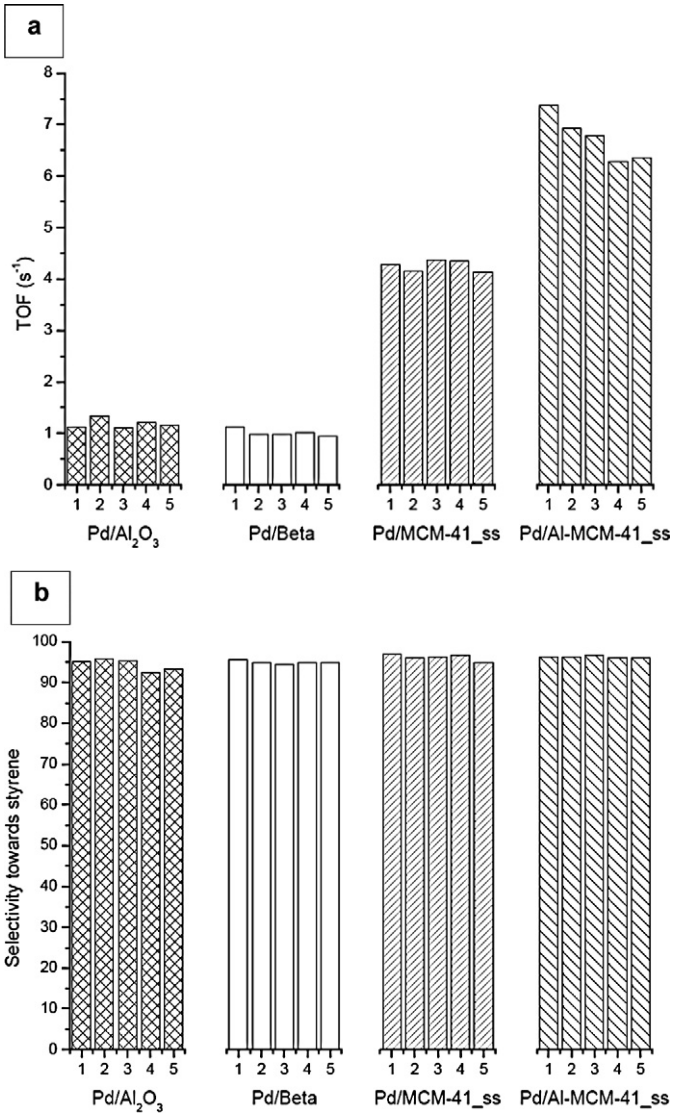

Fig. 6. (a) TOF and (b) selectivity towards styrene of Pd/Al_2O_3, Pd/Beta, Pd/MCM-41_s.s. and Pd/Al-MCM-41_s.s. catalysts in the five consecutive cycles of reutilization of hydrogenation of phenylacetylene.

Pd/Al-MCM-41_s.s., which exhibited fourfold and sixfold higher TOF values, respectively. This finding apparently indicates a relationship between TOF values and palladium nanoparticle size.

Fig. 5 shows the relationship between nanoparticles diameter and TOF values in the first cycle of hydrogenation of phenylacetylene of the different catalysts. As we can see, the TOF values increased with increasing palladium nanoparticle diameter. This is an interesting result, because apart from the innovative simultaneous synthesis method developed in this work, in which MCM-41 and Al-MCM-41 are generated in situ with a colloidal suspension of palladium nanoparticles, in the range of particle diameters studied here, the hydrogenation of phenylacetylene seems to be sensitive to the structure of the catalyst. These findings agree with those of another recent study of the hydrogenation of alkynes [27]. Nevertheless, further efforts will be undertaken to synthesize palladium particles between 3 and 11 nm in diameter to further investigate this area.

Fig. 6 shows five consecutive cycles of reutilization experiments of four of the catalysts (Pd/Al_2O_3, Pd/Beta, Pd/MCM-41_s.s., and Pd/Al-MCM-41_s.s.). Neither the catalytic activity nor the selectivity decreased appreciably in these cycles, except for Pd/Al-MCM-41_s.s. In this case, the nanoparticles could be less well anchored to the support (although a constant value was achieved after the third cycle). Furthermore, the conversion and selectivity shown in the hydrogenation reaction curves could be practically reproduced in the five cycles. Moreover, no Pd leaching from the samples occurred during catalytic applications, as confirmed by inductively coupled plasma (ICP) analysis. These findings conclusively demonstrate the good reusability of all of the supported catalysts.

4. Conclusion

In this paper we have described the preparation of palladium heterogeneous catalysts supported on different inorganic materials. Palladium colloids, prepared by the reduction-by-solvent method, were deposited on four different supports: γ-alumina (Pd/Al_2O_3), zeolite Beta (Pd/Beta), MCM-41, and Al-MCM-41. For the two mesoporous MCM materials, the corresponding catalysts were synthesized by two different methods: incipient wetness and our innovative simultaneous synthesis method, which involves the direct incorporation of palladium nanoparticles into the mesoporous material synthesis solution before hydrolysis of the silica precursor.

The prepared catalysts have proven to be highly active and selective under very mild conditions (323 K, H_2 flow of 30 mL/min, ambient pressure) in the partial hydrogenation of phenylacetylene. The performance of the prepared catalysts was very similar to that of Pd nanoparticles in the homogeneous phase and was significantly greater for the catalysts prepared following the s.s. procedure. The much higher TOF values of these latter catalysts suggest that, in the range of particle diameters studied, the hydrogenation of phenylacetylene is structure-sensitive.

All of the catalysts demonstrated good reusability with no appreciable loss of activity or selectivity throughout a five-cycle operation protocol. No palladium leaching was detected on these samples during or after their use over five reaction cycles, demonstrating the strong interaction between the palladium nanoparticles and the different supports. Thus, these catalysts have been confirmed to be fully reusable, and they represent an interesting alternative to other conventional catalysts.

Acknowledgments

The authors thank the Spanish Ministry of Education and Science (project CTQ2006-08958/PPQ) and the European Union (FEDER Program) for financial support.

References

[1] T. Vergunst, F. Kapteijn, J.A. Moulijn, Ind. Eng. Chem. Res. 40 (2001) 2801.
[2] X. Huang, B. Wilhite, M.J. McCready, A. Varma, Chem. Eng. Sci. 58 (2003) 3465.
[3] J. Silvestre-Albero, F. Rodríguez-Reinoso, A. Sepúlveda-Escribano, J. Catal. 210 (2002) 127.
[4] S.R. de Miguel, M.C. Román-Martínez, D. Cazorla-Amorós, E.L. Jablonski, O.A. Scelza, Catal. Today 66 (2001) 289.
[5] G. Ertl, H. Knözinger, J. Weitkamp, Handbook of Heterogeneous Catalysis, Wiley–VCH, Amsterdam, 1997.
[6] M.E. Davis, Ind. Eng. Chem. Res. 30 (1991) 1675.
[7] C.T. Kresge, M.E. Leonowicz, W.J. Roth, J.C. Vartuli, J.S. Beck, Nature 359 (1992) 710.
[8] S. Domínguez-Domínguez, A. Berenguer-Murcia, D. Cazorla-Amorós, A. Linares-Solano, J. Catal. 243 (2006) 74.
[9] S. Domínguez-Domínguez, A. Berenguer-Murcia, B.K. Pradhan, D. Cazorla-Amorós, A. Linares-Solano, J. Phys. Chem. C 112 (2008) 3827.
[10] M. Grun, K.K. Unger, A. Matsumoto, K. Tsutsumi, Microporous Mesoporous Mater. 27 (1999) 207.
[11] A. Berenguer-Murcia, A.J. Fletcher, J. García-Martínez, D. Cazorla-Amorós, A. Linares-Solano, K.M. Thomas, J. Phys. Chem. B 107 (2003) 1012.
[12] S. Lowell, J.E. Shields, M.A. Thomas, M. Thommes, Characterization of Porous Solids and Powders: Surface Area, Pore Size and Density, Kluver Academic, United States, 2004.
[13] M.M. Dubinin, Chem. Rev. 60 (1960) 235.
[14] D. Cazorla-Amorós, J. Alcañiz-Monge, M.A. de la Casa-Lillo, A. Linares-Solano, Langmuir 14 (1998) 4589.
[15] M. Boudart, Kinetics of Heterogeneous Catalytic Reactions, Princeton Univ. Press, Princeton, NJ, 1984, p. 26.
[16] S.D. Jackson, L.A. Shaw, Appl. Catal. A Gen. 134 (1996) 91.
[17] G. Fagherazzi, P. Canton, P. Riello, N. Pernicone, F. Pinna, M. Battagliarin, Langmuir 16 (2000) 4539.
[18] P. Canton, G. Fagherazzi, M. Battagliarin, F. Menegazzo, F. Pinna, N. Pernicone, Langmuir 18 (2002) 6530.
[19] F. Rouquerol, J. Rouquerol, K. Sing, Adsorption by Powders & Porous Solids: Principles, Methodology and Applications, Academic Press, London, 1999.
[20] K.S.W. Sing, D.H. Everett, R.A.W. Haul, L. Moscou, R.A. Pierotti, J. Rouquerol, T. Siemieniewska, Pure Appl. Chem. 57 (1985) 603.
[21] S. Brunauer, L.S. Deming, W.E. Deming, E. Teller, J. Am. Chem. Soc. 62 (1940) 1723.
[22] E. Díaz, S. Ordóñez, A. Vega, J. Coca, Microporous Mesoporous Mater. 70 (2004) 109.
[23] N. Marín-Astorga, G. Pecchi, J.L.G. Fierro, P. Reyes, J. Mol. Catal. A Chem. 231 (2005) 67.
[24] A. Papp, A. Molnar, A. Mastalir, Appl. Catal. A Gen. 289 (2005) 256.
[25] D. Lee, G.S. Jung, H.C. Lee, J.S. Lee, Catal. Today 111 (2006) 373.
[26] J.M. Newsam, M.M.J. Treacy, W.T. Koetsier, C.B. Degruyter, Proc. R. Soc. London Ser. A Math. Phys. Eng. Sci. 420 (1988) 375.
[27] N. Semagina, A. Renken, L. Kiwi-Minsker, J. Phys. Chem. C 111 (2007) 13933.